DOI: 10.1002/ejic.200800198

Sulfur-Assisted Approach for the Low-Temperature Synthesis of β-SiC Nanowires

Zhicheng Ju,[a] Zheng Xing,[a] Chunli Guo,[a] Lishan Yang,[a] Liqiang Xu,*[a] and Yitai Qian[a]

Keywords: Nanostructures / Crystal growth / Crystal morphology

Silicon carbide (SiC) nanowires coexisting with amorphous graphite particles were initially produced by using silicon powder, tetrachlorethylene, metallic Na, and sulfur powder as reactants in an autoclave at 130 °C. Pure β-SiC could be finally obtained after heating the sample in concentrated H_2SO_4 by refluxing at 180 °C, which was proved by the X-ray powder diffraction patterns. Transmission electron microscopy (TEM) images and scanning electron microscope (SEM) images show that the product is mainly composed of SiC nanowires (over 75 %) with an average diameter of about of 30 nm and lengths up to tens of micrometers. High-resolution TEM shows that the nanowires have preferential growth along the [111] direction. It was found that when sulfur was absent, crystalline β-SiC powders could not be obtained unless the target temperature was raised higher than 270 °C. In the mean time, the ratio of the nanowires also dropped dramatically (≈20 %). The effects of sulfur, reaction time, and temperature on the morphologies of the final products, together with the properties of the final products, were also discussed.

Introduction

Silicon carbide ceramic materials have excellent mechanical properties, high physical and chemical stability, and high thermal conductivity.[1] In addition, silicon carbide is an important wide bandgap (2.39 eV for 3C–SiC at room temperature)[2] material, which has been widely applied as a high-temperature semiconductor.[3] Recently, various techniques such as carbon nanotube confined growth,[4] chemical vapor deposition,[5] sol–gel techniques,[6] and arc discharge[7] have been used for the synthesis of silicon carbide nanocrystals, especially one-dimensional (1D) SiC nanomaterials, These methods have been successfully used to synthesize pure SiC nanorods or nanowires by using temperatures above 1000 °C.

New convenient routes have also been utilized to prepare SiC nanomaterials. For example, β-SiC whiskers were produced by thermal decomposition of sulfur-containing silicone oils.[8] In another report, an amorphous precursor was first synthesized by coreduction of $SiCl_4$ and CCl_4 in a nonpolar solvent at 130 °C, and crystalline SiC was then obtained by posttreatment at 1450–1750 °C.[9] Similar reactions were reported for the synthesis of β-SiC nanorods in autoclaves at 400 °C.[10]

[a] Key Laboratory of Colloid and Interface Chemistry, Ministry of Education, School of Chemistry and Chemical Engineering, Shandong University,
Jinan 250100, P. R. China
Fax: +86-531-88366280
E-mail: xulq@sdu.edu.cn

In this study, a sulfur-assisted reduction route was developed for the synthesis of β-SiC nanowires (with an average diameter of ≈30 nm and lengths up to tens of micrometers) at low temperature in an autoclave. The as-obtained product contains a very small amount of amorphous graphite, which can be removed by prolonged heating of a solution of the sample in concentrated H_2SO_4 at reflux (other convenient routes can also eliminate the residual carbon, including repetition of the extraction process by employing bromoform to separate the SiC and graphite or calcination of the product at 600 °C for 3 h in air). Almost all of the SiC nanowires maintained their 1D shape and size after the purification process, and the output of SiC was ≈70% based on the amount of Si powder.

Results and Discussion

Figure 1 show the typical XRD patterns of the products. Curve a is the XRD pattern of the product synthesized by heating the sample at 130 °C for 40 h, followed by subsequent washing with absolute alcohol, 1 M HCl, and distilled water. In this pattern, Si and amorphous graphite were found to coexist with β-SiC. Curve b shows the XRD pattern of the composite obtained after it was heated at reflux in concentrated H_2SO_4; only β-SiC and small amounts of Si were found, whereas no residual carbon was observed. Curve c demonstrates that only β-SiC was left after the refluxing process (in concentrated H_2SO_4) and repeated washing with dilute HF. Curve d shows the XRD pattern of the product obtained after calcination (at 600 °C

for 3 h in air) and further purification by repeated washing with dilute HF; all of the diffraction peaks could be assigned to β-SiC. The strong intense peaks centered at 2θ = 35.70, 41.41, 60.01, 71.78, and 75.52° could be respectively indexed as the (111), (200), (220), (311), and (222) reflections of β-SiC with lattice constant of a = 4.36 Å (JCPDS, card No.75-0254). No other impurities were detected in these patterns. The strong and sharp peaks indicated that the samples were well crystalline. In addition, it was found that peak (111) is the only peak that gains a substantial increase in relative intensity, indicating that the nanowires may have a preferential growth orientation along the [111] direction.

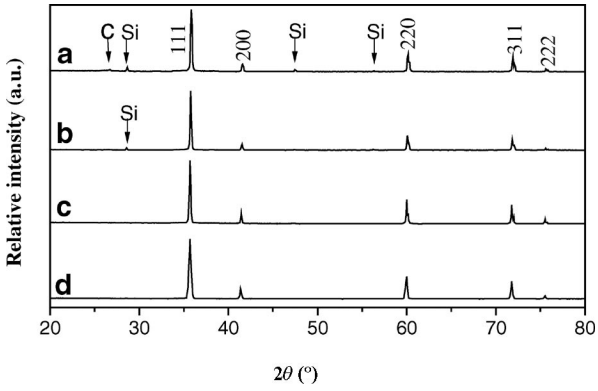

Figure 1. XRD patterns of the powder synthesized by heating the sample at 130 °C for 40 h: (a) Purified by ethanol, 1 M HCl, and distilled water; (b) heated at reflux in concentrated H_2SO_4 at 180 °C for 6 h; (c) heated at reflux in concentrated H_2SO_4 at 180 °C for 6 h, then washed several times with dilute HF; (d) product obtained after calcination (at 600 °C for 3 h in air) and further purification by washing several times with dilute HF.

The structure and morphology of the as-obtained products were further observed by TEM, SAED, and HRTEM. Figure 2a shows a typical TEM image of the purified products (produced by treatment at 130 °C for 40 h), which indicates that the sample is composed of randomly distributed 1D nanostructures with uniform diameters of about 30 nm and lengths up to tens of micrometers. Figure 2b shows the image of the sample obtained after repeated extraction (with bromoform) and further purification by washing several times with dilute HF, and Figure 2c shows the image of the sample obtained after calcination at 600 °C for 3 h in air. When Figure 2a is compared with Figure 2b,c it is clear that almost no change in the morphology and diameter of the sample occurred during purification. The yield of SiC nanowires is estimated to be over 75% on the basis of the TEM view. The inset at the bottom left-hand corner of Figure 2a (or Figure 2c) shows a typical SAED pattern of an individual nanowire, revealing its single-crystalline nature. Moreover, the SAED patterns taken from different positions along the nanowire (without tilting the sample with respect to the electron beam) are found to be almost identical. This indicates that the entire nanowire is a single crystal. Figure 2d shows the HRTEM image of part of a randomly selected nanowire: the regularly arranged lattice fringes can be clearly seen, which reveals its high crystallinity. The interplanar spacing is about 0.25 nm, which corresponds to (111) spacing of β-SiC. In addition, the [111] direction is parallel to the axis of the nanowire, indicating that the nanowire grows along the [111] direction, which is consistent with the XRD results.

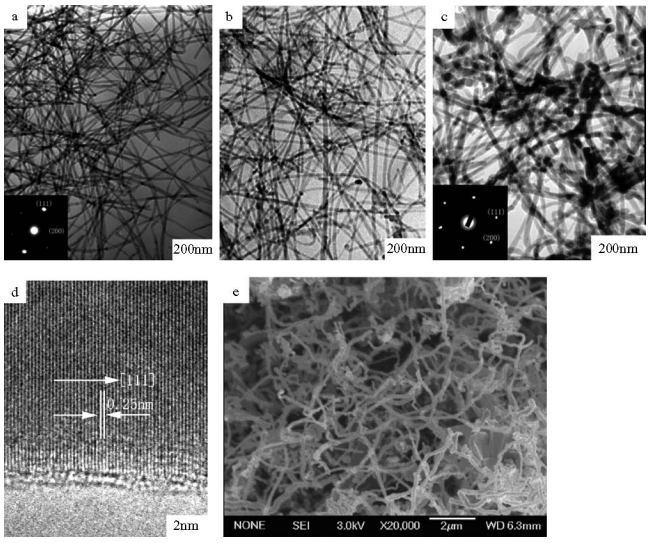

Figure 2. TEM images of the powder synthesized by heating the sample at 130 °C for 40 h: (a) general low-magnification TEM image and inset is a typical SAED pattern: heated at reflux in concentrated H_2SO_4 at 180 °C for 6 h, and after repeated washing with dilute HF; (b) TEM image: repeated extraction with bromoform and repeated washing with dilute HF; (c) TEM image with a typical SAED pattern: calcined at 600 °C for 3 h in air and repeated washing with dilute HF; (d) HRTEM image of part of a single nanowire; (e) typical low-magnification FESEM image of the β-SiC nanowires.

The morphology and dimensions of the as-prepared sample were further characterized by FESEM, and typical images are shown in Figure 2e (obtained after treatment at 130 °C for 40 h). Besides the irregular particles, the proportion of the nanowires with diameters of about 30 nm in the product is approximately 75%. This result is in good agreement with those of the statistical TEM observations.

In order to investigate the effect of reaction time and temperature on the formation of crystalline SiC, we also performed the following comparative experiments. Figure 3a shows the XRD pattern of the powder synthesized by heating the sample at 130 °C for 20 h (obtained after purification). It exhibits broad diffraction peaks and weak diffraction intensity. In this experiment, the heating temperature should be no less than 100 °C, otherwise no crystalline SiC is detected in the products, as can be seen in Figure 3b. If S powder was absent, the reaction temperature should be raised higher than 270 °C in order to produce crystalline β-SiC (Figure 3c) powder. As evidenced by Figure 3d, only Si and amorphous carbon were produced at 250 °C after 40 h.

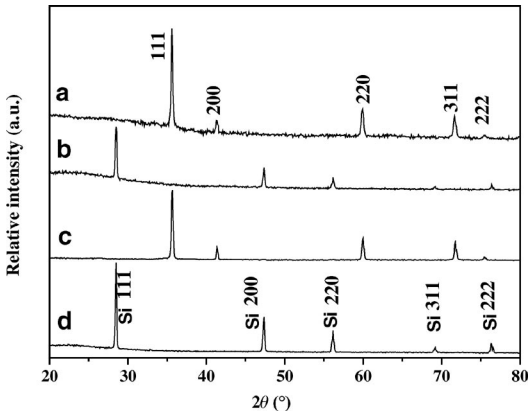

Figure 3. XRD patterns of different reaction conditions (a) 130 °C, 20 h; (b) 100 °C, 40 h; (c) 270 °C, 20 h and without S powder; (d) 250 °C, 40 h and without S powder.

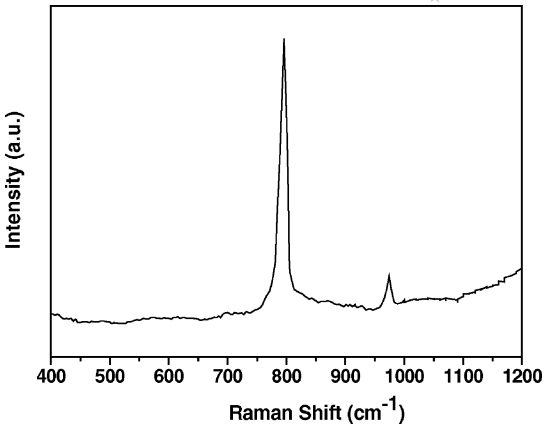

Figure 5. Raman spectrum of the relatively pure β-SiC samples prepared by heating the sample at 130 °C for 40 h.

The room-temperature photoluminescence (PL) spectra of the obtained β-SiC are shown in Figure 4. Curves a and b show the PL spectrum of samples 1 and 2, and peaks with strong intensity are clearly observed at 442 and 439 nm, respectively. In comparison to the previously reported PL spectra of β-SiC nanowires[11] or films,[12] the emission peaks for the β-SiC product is obviously blue-shifted. Recently, various emission wavelengths from β-SiC nanostructures have been reported,[6a,11,13] indicating that the luminescence characteristics depend strongly on the β-SiC nanostructures that were produced through different approaches. Therefore, we consider that the different optical performances of the as-prepared samples might be attributed to their different shapes and sizes.[5f–5h,14]

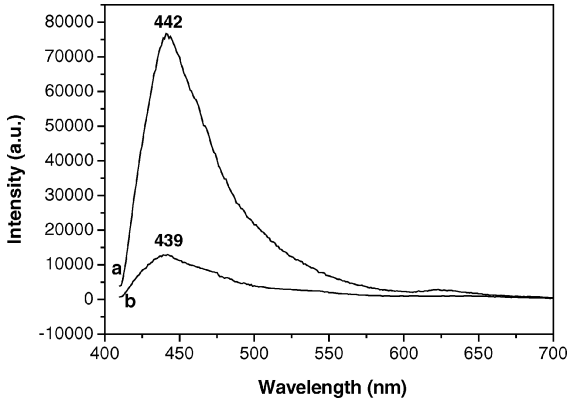

Figure 4. Room-temperature photoluminescence spectra of the β-SiC samples obtained by heating the sample at: (a) 130 °C for 40 h and (b) 270 °C after 20 h in the absence of S powder.

A typical Raman spectrum taken from the SiC product (obtained at 130 °C, 40 h) is shown in Figure 5. There are two peaks centered around 796.6 and 974.1 cm^{-1}, which correspond to the TO and LO phonons at the Γ point of β-SiC, respectively.[5f,5h,5j,5k,15] The sharp peaks confirm that the as-synthesized β-SiC nanostructures are well crystalline.[16] These results are consistent with the X-ray patterns and the HRTEM observations.

TGA was carried out under a flow of air in the temperature range of 200–1000 °C (see Figure 6) in order to study the thermal stabilities of the samples. Initially, it is observed from the TGA curves that there is a slight weight loss, which might be attributed to the loss of water that absorbed on the surface of the SiC sample. A gradual small weight gain was observed above 800 °C, suggesting that SiC is oxidized in the air atmosphere, which is in agreement with previous reports.[16] Relative to curve b, curve a has a larger weight gain (7.48% for curve a, 3.37% for curve b at 1000 °C), probably because smaller particle sizes accordingly have greater surface areas, which results in their vulnerability to oxidation. At the same time, the SiC sample did not undergo any drastic weight gain or loss in the temperature range 200–1000 °C. This result was consistent with the reported values.[17]

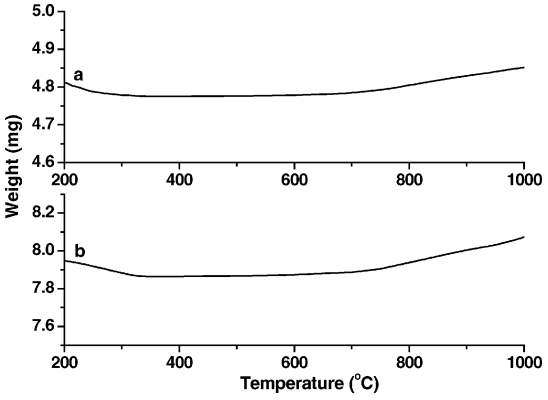

Figure 6. TGA analysis of the SiC sample carried out in air at a heating rate of 5 °C min^{-1}: (a) obtained by heating the sample at 130 °C for 40 h; (b) obtained by heating the sample at 270 °C for 20 h without S powder.

To study the influences of the reactants on the formation and yield of β-SiC nanowires, we carried out a series of experiments (Table 1) with processes similar to that mentioned in the Experimental Section.

Table 1. Products obtained under different experimental conditions (ratios of the nanowires were estimated through statistical SEM and TEM observation of the products).

Exp. no.	Sulfur [g]	Temperature [°C]	Time [h]	Nanowire contents [%]
1	1.0	130	20	50
2	1.0	130	30	70
3	1.0	130	40	75
4	2.0	130	40	70
5	0.5	130	40	50
6	—	130	40	–
7	1.0	150	40	70
8	1.0	250	40	70
9	—	270	20	20
10	—	250	40	–

From experiment 1, it was found that the products mainly contain nanowires (about 50%) and irregular particles (not presented). The yield of SiC nanowires increases with prolonged reaction time (Table 1, experiment 2). The ratio of ca. 75% SiC nanowires can be obtained from experiment 3 (Table 1, Figure 2a). At the same time, as the amount of S was increased or decreased, the yield of SiC nanowires decreased (Table 1, experiments 4 and 5). If sulfur was absent from the reaction system, the crystalline SiC could not be obtained at 130 °C (Table 1, experiment 6) but was formed at temperatures above 270 °C (Table 1, experiment 9). Nevertheless, the yield of nanowires is very low and their diameters are not uniform. When the reaction temperature is lower than 250 °C without the input of S powder, we could not obtain crystalline SiC (Table 1, experiment 10). As evidenced by the above experiments, the proper ratio of sulfur is a vital factor for the low-temperature formation of crystalline SiC nanowires.

According to the aforementioned experimental results, the overall reaction involved in this experiment may be tentatively written (at 130 °C) as Equation (1).

$$2\ Si\ (s) + S\ (l) + C_2Cl_4\ (v) + 6\ Na\ (l) \rightarrow 2\ SiC\ (s) + Na_2S\ (s) + 4\ NaCl\ (s) \quad (1)$$

According to the calculated results of Gibbs free energy, the reaction is thermodynamically spontaneous (ΔrG_1° = –2022.74 kJ mol^{-1}, ΔrH_1° = –2141.54 kJ mol^{-1}).
At 130 °C, in the absence of sulfur powder the reaction can be written as Equation (2).

$$2\ Si\ (s) + C_2Cl_4\ (v) + 4\ Na\ (l) \rightarrow 2\ SiC\ (s) + 4\ NaCl\ (s) \quad (2)$$

where

ΔrG_2° = –1672.68 kJ mol^{-1}, ΔrH_2° = –1775.88 kJ mol^{-1}

At 270 °C, in the absent of sulfur powder the reaction is that outlined in Equation (3).[17]

$$2\ Si\ (s) + C_2Cl_4\ (v) + 4\ Na\ (l) \rightarrow 2\ SiC\ (s) + 4\ NaCl\ (s) \quad (3)$$

where

ΔrG_3° = –1636.56 kJ mol^{-1}, ΔrH_3° = –1774.80 kJ mol^{-1}

From comparison of the ΔrG° values of these three overall reactions, it is clear that reaction 1 is thermodynamically most favorable.

Besides the effect of sulfur, the reaction temperature is also an important factor in SiC nanowire formation. If the reaction temperature is increased while the other conditions are kept constant, SiC nanowires could be obtained in large quantity (Table 1, experiments 7 and 8). The yield of SiC was found to increase slightly but the proportion of nanowires decreased slightly with an increase in the temperature (for example, 150 °C or 250 °C), and their diameters were also found to change slightly (≈20–50 nm at 150 °C and 30–70 nm at 250 °C, respectively).

Figure 7 display the typical XRD pattern of the raw product (without posttreatment) obtained by heating the sample at 130 °C for 40 h; the diffraction peaks could be assigned to SiC, NaCl, Si, and Na_2S. The morphology of the SiC nanowires (without posttreatment) was also investigated. It is occasionally observed that large nanoparticles were attached to the tips of the SiC nanowires, and a typical FSEM image of part of an individual SiC nanowire is shown in Figure 8a. Figure 8b is the corresponding EDX spectrum of the part arrowed in Figure 8a, indicating that it is composed of Na_2S and SiC and to a lesser extent NaCl (based on the results of XRD pattern shown in Figure 7).

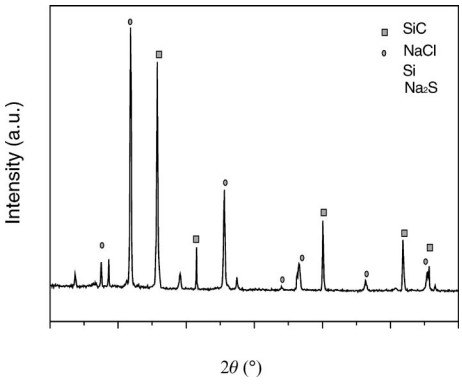

Figure 7. Typical XRD pattern of the 3C-SiC powder synthesized by heating the sample at 130 °C for 40 h without any posttreatment; the diffraction peaks could be assigned to SiC, NaCl, Si, and Na_2S (SiC, JCPDS card No. 75-0254; NaCl: JCPDS card No. 05-0628; Si: JCPDS card No. 27-1402; Na_2S, JCPDS card No. 65-2995).

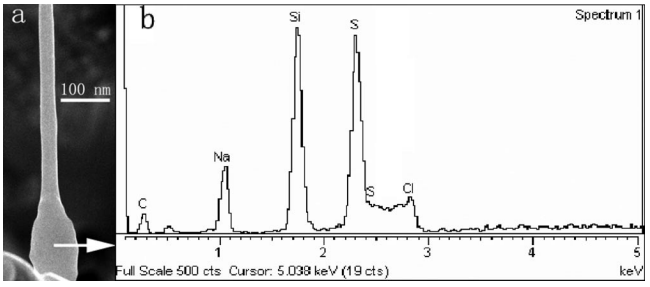

Figure 8. (a) Typical SEM image of an individual nanowire without posttreatment, (b) EDX spectrum taken from the part as-arrowed in Figure 8a.

In this experiment, the reactants used here have relatively low melting points or boiling points: Na m.p. 97.8 °C, C_2Cl_4 b.p. 121.2 °C, and sulfur m.p. 115 °C. With a gradual increase in reaction temperature, Na (acting as a strong reductant) will gradually react with C_2Cl_4 vapor to form active carbon (C) atoms (which will react with Si to form SiC nanowires) and NaCl. At the same time, S would liquefy and react with Na to form Na_2S. Combined, the results of the XRD pattern (Figure 7), FSEM image (Figure 8), and the contrasting experimental results (with or without S powder addition), it is more likely that Na_2S plays a catalytic role in the formation of SiC nanowires, and the formation mechanism of 3C-SiC nanowires is perhaps analogous to the vapor–liquid–solid (VLS) growth process.[18] In contrast, Na_2S is more prone to form than SiS or SiS_2 according to the calculated values of their Gibbs free energy; however, the possible production and effect of silicon sulfides such as SiS or SiS_2 on the final formation of the SiC nanowires cannot not be completely excluded.[19] Although much work is still required to control the reaction kinetics and to understand the formation process of SiC nanowires, we believe that this method could be used, in principle, to produce other silicides and nitrides at low temperature.

Conclusion

A sulfur-assisted chemical reduction route was developed for the synthesis of β-SiC nanowires (with an average diameter of ≈30 nm and lengths up to tens of micrometers) at 130–180 °C. The yield of SiC nanowires is estimated to be over 75% based on the TEM view. TEM, SAED, and HREM analyses confirm that the nanowire is single-crystalline and that the growth direction is along [111]. In the absence of S powder, the reaction temperature should be above 270 °C in order to obtain crystalline SiC. In comparison to other processes, our method is a simple way to synthesize silicon carbide nanopowders with a relatively low cost.

Experimental Section

General: All the chemical reagents were of analytical purity and purchased from Shanghai Chemical Reagents Company.

Preparation of the Sample 1: Typically, C_2Cl_4 (3 mL), Si powder (1.0 g), S powder (1.0 g), and an excess amount of metal Na (4.0 g) were loaded into a 20-mL stainless-steel autoclave, which was then put into an oven. The temperature of the oven was raised from room temperature to 130 °C at a rate of about 10 °C min^{-1} and then maintained at 130 °C for 40 h. After that, the autoclave was cooled to room temperature naturally, and the products in the autoclave were collected and washed with absolute alcohol and 1 M HCl. The sample was then heated at reflux in concentrated H_2SO_4 (or $HClO_4$, 70 wt.-%) at 180 °C for 6 h to eliminate the residual carbon (other convenient routes to eliminate the residual carbon include repetition of the extraction process by employing bromoform to separate the SiC and graphite or calcination of the product at 600 °C for 3 h in air) and finally treated with dilute HF and distilled water to remove Si and other impurities. The acquired sample was then dried under vacuum at 60 °C for 5 h to afford a gray product.

Preparation of the Sample 2: When S powder was absent but keeping other reagents unchanged, crystalline sample 2 could be obtained only when the reaction temperature was maintained at or above 270 °C for 20 h.

Sample Characterization: X-ray powder diffraction (XRD) patterns of the products were recorded with a Bruker D8 advanced X-ray diffractometer equipped with Ni-filtered Cu-K_α radiation (λ = 1.5418 Å). Transmission electron microscopy (TEM) images were taken with a Hitachi H-600 transmission electron microscope by using an accelerating voltage of 100 kV. High-resolution transmission electron microscopy (HRTEM) images and the selected area electron diffraction (SAED) patterns were taken with a JEOL-2100 transmission electron microscope. Scanning electron microscope (SEM) images were recorded with a JEOL JSM-6700F field emission electron microscope. PL spectrum measurement was performed with an Edinburgh instruments FLS920 fluorescence spectrophotometer with a Xe lamp at room temperature. The excitation wavelength was 367 nm and the filter wavelength was 430 nm. Raman spectra were recorded at ambient temperature with a NEXUS 670 FTIR Raman spectrometer. Thermal gravimetric analysis (TGA) was recorded with a Mettler Toledo TGA/SDTA851 thermal analyzer apparatus under air flow.

Acknowledgments

This work was supported by National Natural Science Foundation of China (No.20671058, 20701026), the 973 Project of China (No. 2005CB623601), and Tai-Shan Scholar Project of Shandong Province.

[1] a) P. Kim, C. M. Lieber, *Science* **1999**, *286*, 2148–2150; b) W. Yang, H. Araki, C. Tang, S. Thaveethavorn, A. Kohyama, H. Suzuki, T. Noda, *Adv. Mater.* **2005**, *17*, 1519–1523; c) P. F. Becher, C. H. Hsueh, P. T. T. N. Angelini, *J. Am. Ceram. Soc.* **1988**, *71*, 1050–1061.

[2] a) J. A. Powell, L. G. Matus, M. A. Kuczmarski, *J. Electrochem. Soc.* **1987**, *134*, 1558–1565; b) Y. Li, P. S. Dorozhkin, Y. Bando, D. Golberg, *Adv. Mater.* **2005**, *17*, 545–549; c) H. K. Seong, H. J. Choi, S. K. Lee, J. I. Lee, D. J. Choi, *Appl. Phys. Lett.* **2004**, *85*, 1256–1258.

[3] a) Z. L. Wang, Z. R. Dai, R. P. Gao, Z. G. Bai, *Appl. Phys. Lett.* **2000**, *77*, 3349–3351; b) A. Fisher, B. Schroter, W. Richer, *Appl. Phys. Lett.* **1995**, *66*, 3182–3184; c) J. C. Li, S. T. Lee, *Chem. Phys. Lett.* **2002**, *355*, 147–150.

[4] a) H. J. Dai, E. W. Wong, Y. Z. Lu, S. S. Fan, C. M. Lieber, *Nature* **1995**, *375*, 769–772; b) W. Q. Han, S. S. Fan, Q. Q. Li, W. J. Liang, B. L. Gu, D. P. Yu, *Chem. Phys. Lett.* **1997**, *265*, 374–378; c) A. I. Kharlamov, S. V. Loichenko, N. V. Kirillova, V. V. Fomenko, M. E. Bondarenko, Z. A. Zaitseva, *Inorg. Mater.* **2003**, *39*, 260–265; d) Y. Xia, P. Yang, Y. Sun, Y. Wu, B. Mayers, B. Gates, Y. Yin, F. Kim, H. Han, *Adv. Mater.* **2003**, *15*, 353–389; e) C. C. Tang, S. S. Fan, H. Y. Dang, J. H. Zhao, Z. Zhang, P. Li, Q. Gu, *J. Cryst. Growth* **2000**, *210*, 595–599.

[5] a) X. T. Zhou, N. Wang, H. L. Lai, H. Y. Peng, I. Bello, N. B. Wang, S. T. Lee, *Appl. Phys. Lett.* **1999**, *74*, 3942–3944; b) H. F. Zhang, C. M. Wang, L. S. Wang, *Nano Lett.* **2002**, *2*, 941–944; c) X. H. Sun, C. P. Li, W. K. Wong, N. B. Wong, C. S. Lee, S. T. Lee, B. K. Teo, *J. Am. Chem. Soc.* **2002**, *124*, 14464–14471; d) Y. B. Li, P. S. Dorozhkin, Y. Bando, D. Golberg, *Adv. Mater.* **2005**, *17*, 545–549; e) G. Z. Shen, Y. Bando, D. Golberg, *Cryst. Growth Des.* **2007**, *7*, 35–38; f) J. J. Niu, J. N. Wang, *J. Phys. Chem. B* **2007**, *111*, 4368–4373; g) R. B. Wu, Y. Pan, G. Y.

Yang, M. X. Gao, L. L. Wu, J. J. Chen, R. Zhai, J. Lin, *J. Phys. Chem. C* **2007**, *111*, 6233–6237; h) Z. J. Li, J. L. Zhang, A. L. Meng, J. Z. Guo, *J. Phys. Chem. B* **2006**, *110*, 22382–22386; i) Y. F. Zhang, X. D. Han, K. Zheng, Z. Zhang, X. N. Zhang, J. Y. Fu, Y. Ji, Y. J. Hao, X. Y. Guo, Z. L. Wang, *Adv. Funct. Mater.* **2007**, *17*, 3435–3440; j) B. Mikhael, B. Arnaud, C. David, F. Gabriel, M. Philippe, *Adv. Funct. Mater.* **2007**, *17*, 939–943; k) G. S. Siddarth, V. D. Albert, D. V. Mark, L. Igor, E. M. James, T. Yong-Lai, V. R. Mulpuri, *Chem. Mater.* **2007**, *19*, 5531–5537; l) J. J. Niu, J. N. Wang, *Eur. J. Inorg. Chem.* **2007**, 4006–4010; m) C. H. Wang, H. K. Lin, T. Y. Ke, T. J. Palathinkal, N. H. Tai, I. N. Lin, C. Y. Lee, H. T. Chiu, *Chem. Mater.* **2007**, *19*, 3956–3962.

[6] a) G. Gundiah, G. V. Madhav, A. Govindaraj, M. Sheikh, C. N. R. Rao, *J. Mater. Chem.* **2002**, *12*, 1606–1611; b) G. W. Meng, L. D. Zhang, C. M. Mo, S. Y. Zhang, Y. Qin, S. P. Feng, H. J. Li, *J. Mater. Res.* **1998**, *13*, 2533–2538; c) C. H. Liang, G. W. Meng, L. D. Zhang, Y. C. Wu, Z. Cu, *Chem. Phys. Lett.* **2000**, *329*, 323–328.

[7] a) T. Seeger, P. Kohler-Redlich, M. Ruhle, *Adv. Mater.* **2000**, *12*, 279–282; b) Y. B. Li, S. S. Xie, X. P. Zou, D. S. Tang, Z. Q. Liu, W. Y. Zhou, G. J. Wang, *J. Cryst. Growth* **2001**, *223*, 125–128.

[8] H. Katsuki, H. Ushijima, M. Kanda, H. Iwanaga, M. Egashira, *Yogyo-Kyokai-Shi* **1987**, *95*, 1089–1091.

[9] J. J. Ritter, *Adv. Ceram.* **1987**, *21*, 21–31.

[10] Q. Y. Lu, J. Q. Hu, K. B. Tang, Y. T. Qian, *Appl. Phys. Lett.* **1999**, *75*, 507–509.

[11] J. Q. Hu, Q. Y. Lu, K. B. Tang, B. Deng, R. R. Jiang, Y. T. Qian, W. C. Yu, G. E. Zhou, X. M. Liu, J. X. Wu, *J. Phys. Chem. B* **2000**, *104*, 5251–5254.

[12] H. W. Shim, K. C. Kim, Y. H. Seo, K. S. Nahm, E. K. Suh, H. J. Lee, Y. G. Hwang, *Appl. Phys. Lett.* **1997**, *70*, 1757–1759.

[13] X. L. Wu, J. Y. Fan, T. Qiu, X. Yang, G. G. Siu, P. K. Chu, *Phys. Rev. Lett.* **2005**, *94*, 026102.

[14] a) S. Nie, S. R. Emory, *Science* **1997**, *275*, 1102–1106; b) S. Link, M. A. El-Sayed, *J. Phys. Chem. B* **1999**, *103*, 8410–8426.

[15] a) L. Geng, J. Zhang, *Mater. Chem. Phys.* **2004**, *84*, 243–246; b) D. Olego, M. Cardona, *Phys. Rev. B* **1982**, *25*, 3889–3896; c) Z. C. Feng, A. J. Mascarenhas, W. J. Choyke, J. A. Powell, *J. Appl. Phys.* **1998**, *64*, 3176–3186.

[16] a) Z. X. Yang, Y. D. Xia, M. Robert, *Chem. Mater.* **2004**, *16*, 3877–3884; b) R. Moene, M. Makkee, J. A. Moulijn, *Appl. Catal. A* **1998**, *167*, 321–330.

[17] T. Tomita, S. Saito, M. Baba, M. Hundhausen, T. Suemoto, S. Nakashima, *Phys. Rev. B* **2000**, *62*, 12896–12901.

[18] a) R. S. Wagner, W. C. Ellis, *Appl. Phys. Lett.* **1964**, *4*, 89–92; b) H. J. Dai, E. W. Wong, Y. Z. Lu, S. S. Fan, C. M. Lieber, *Nature* **1995**, *375*, 769–772; c) C. H. Liang, G. W. Meng, L. D. Zhang, Y. C. Wu, Z. Cui, *Chem. Phys. Lett.* **2000**, *329*, 323–328; d) M. S. Gudiksen, C. M. Lieber, *J. Am. Chem. Soc.* **2000**, *122*, 8801–8802; e) Y. Cui, L. J. Lauhon, M. S. Gudiksen, *Appl. Phys. Lett.* **2001**, *78*, 2214–2216.

[19] P. E. D. Morgan, E. A. Pugar, *J. Am. Ceram. Soc.* **1985**, *68*, 699–703.

Received: February 24, 2008
Published Online: July 14, 2008

